

## Improvement in thin cirrus retrievals using an emissivity-adjusted CO<sub>2</sub> slicing algorithm

Hong Zhang

Cooperative Institute for Meteorological Satellite Studies, Space Science and Engineering Center, University of Wisconsin-Madison, Madison, Wisconsin, USA

W. Paul Menzel

Office of Research and Applications, National Oceanic and Atmospheric Administration National Environmental Satellite Data and Information Service, Madison, Wisconsin, USA

Received 6 July 2001; revised 6 December 2001; accepted 25 January 2002; published 10 September 2002.

[1] CO<sub>2</sub> slicing has been generally accepted as a useful algorithm for determining cloud top pressure (CTP) and effective cloud amount (ECA) for tropospheric clouds above 600 hPa. To date, the technique has assumed that the surface emissivity is that of a blackbody in the long-wavelength infrared radiances and that the cloud emissivities in spectrally close bands are approximately equal. The modified CO<sub>2</sub> slicing algorithm considers adjustments of both surface emissivity and cloud emissivity ratio. Surface emissivity is adjusted according to the surface types. The ratio of cloud emissivities in spectrally close bands is adjusted away from unity according to radiative transfer calculations. The new CO<sub>2</sub> slicing algorithm is examined with Moderate Resolution Imaging Spectroradiometer (MODIS) Airborne Simulator (MAS) CO<sub>2</sub> band radiance measurements over thin clouds and validated against Cloud Lidar System (CLS) measurements of the same clouds; it is also applied to Geostationary Operational Environmental Satellite (GOES) Sounder data to study the overall impact on cloud property determinations. For high thin clouds an improved product emerges, while for thick and opaque clouds there is little change. For very thin clouds, the CTP increases by about 10–20 hPa and RMS (root mean square bias) difference is approximately 50 hPa; for thin clouds, the CTP increase is about 10 hPa bias and RMS difference is approximately 30 hPa. The new CO<sub>2</sub> slicing algorithm places the clouds lower in the troposphere.

*INDEX TERMS:* 3359 Meteorology and Atmospheric Dynamics: Radiative processes; 3360 Meteorology and Atmospheric Dynamics: Remote sensing; 3394 Meteorology and Atmospheric Dynamics: Instruments and techniques; *KEYWORDS:* modified CO<sub>2</sub> slicing, thin cirrus, cloud emissivity, surface emissivity

**Citation:** Zhang, H., and W. P. Menzel, Improvement in thin cirrus retrievals using an emissivity-adjusted CO<sub>2</sub> slicing algorithm, *J. Geophys. Res.*, 107(D17), 4327, doi:10.1029/2001JD001037, 2002.

### 1. Introduction

[2] The CO<sub>2</sub> slicing algorithm [Smith *et al.*, 1974; Chahine, 1974; Smith and Platt, 1978; Menzel *et al.*, 1983] has been used extensively to infer cirrus cloud top pressure (CTP) and effective cloud amount (ECA, which is the product of cloud emissivity and cloud fraction). The method uses adjacent infrared channels in the CO<sub>2</sub> absorption band and has been shown to be accurate for clouds at pressures less than approximately 600 hPa (i.e., above 4 km). The technique has been applied operationally to 15- $\mu$ m data from such satellite instruments as the High Resolution Infrared Radiometer Sounder (HIRS) [Wylie and Menzel, 1999], the Geostationary Operational Environmental Satellite (GOES) VISSR Atmospheric Sounder (VAS) [Wylie and Menzel, 1989], the GOES Sounder, and the Moderate Resolution Imaging Spectroradi-

ometer (MODIS). As noted in error analyses by Wielicki and Coakley [1981], Menzel *et al.* [1992], and Baum and Wielicki [1994], the errors in the retrieved properties increase with decreasing ECA values, i.e., for optically thin cirrus. The motivation for the current study is to suggest a way to improve the retrievals for optically thin cirrus, namely by exploring the use of emissivity adjustments. Typical assumptions used in the CO<sub>2</sub> slicing algorithm are that the surface emissivity is that of a blackbody in the longwave infrared (IR) radiances and that the cloud emissivities of spectral pairs in the 15- $\mu$ m bands are approximately equal. In this study, we reconsider the treatment of both surface emissivity and cloud emissivity accorded to the 15- $\mu$ m bands.

[3] Among the basic assumptions in the CO<sub>2</sub> algorithm are that (1) the Earth's surface is considered to be a blackbody emitter; (2) the frequencies in all CO<sub>2</sub> band pairs used in the CO<sub>2</sub> slicing algorithm are close enough so that emissivity of the cloud is the same in both bands, (3) the cloud occupies a single layer in the field of view of the

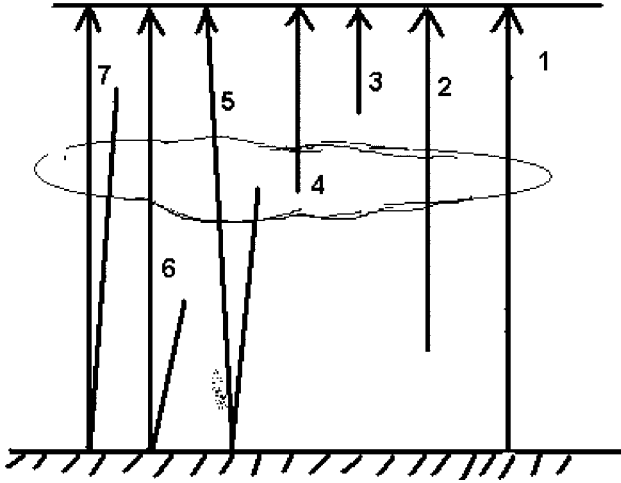


**Figure 1.** A schematic of each contribution measured by the satellite radiometer. The numbers correspond to equation (4).

instrument, and (4) the cloud is infinitesimally thin. In this study, the CO<sub>2</sub> slicing algorithm is adjusted to account for nonblackbody surface emissivity and to allow cloud emissivity ratios to be other than one. Improvements in the CO<sub>2</sub> slicing results for thin cirrus are demonstrated through comparisons of retrievals from the MODIS Airborne Simulator (MAS [King *et al.*, 1996]) with lidar results from the Cloud Lidar System (CLS [Spinhirne and Hart, 1990]). Both instruments were flown on the NASA ER-2 aircraft during the SUCCESS field campaign held in the central United States in April–May 1996. The real time GOES 8 Sounder data were tested for the adjusted CO<sub>2</sub> slicing method.

[4] Section 2 describes the theoretical basis for the CO<sub>2</sub> slicing approach including the emissivity adjustments. Section 3 shows detailed comparisons between the MAS and CLS data. Detailed case studies involving GOES analyses are presented in section 4. Section 5 lists some conclusions.

## 2. CO<sub>2</sub> Slicing Technique With $\epsilon_s$ and $\epsilon_c$ Ratio

[5] Infrared radiation observations used by the CO<sub>2</sub> slicing are affected by surface emissivity and cloud emissivity considerations. When the surface emissivity is less than 1.0, there are two effects that must be considered: (1) the atmospheric radiation is reflected from the surface and (2) the surface emission is reduced from that of a blackbody.

[6] For a specific infrared spectral band, the clear-sky upwelling radiance measured by the satellite within an instrument field-of-view (FOV) can be expressed as

$$R_{clr} = \epsilon_s B_s \tau_s + \int_{p_s}^{p_0} B(T(p)) d\tau + (1 - \epsilon_s) \tau_s \int_{p_0}^{p_s} B(T(p)) d\tau^\perp \quad (1)$$

where subscript  $s$  denotes surface,  $\epsilon_s$  is surface emissivity,  $B_s$  is Planck radiance from the surface,  $p_s$  is surface pressure,  $p_0$  is pressure at the top of the atmosphere,  $\tau_s$  is transmittance from surface to the top of atmosphere,  $B$  is Planck radiance (from atmosphere of pressure  $p$ ),  $\tau$  is the atmospheric transmittance function of radiation of the frequency emitted from the atmospheric pressure level ( $p$ )

arriving at the top of the atmosphere, and  $\tau^\perp$  is transmittance down from the atmosphere pressure level ( $p$ ) to the surface, where  $\tau^\perp = \tau_s / \tau$ .

[7] The first term ( $\epsilon_s B_s \tau_s$ ) on the right-hand side in the above radiative transfer equation (RTE) is the surface emission contribution that depends primarily upon the nature of the surface and the surface radiance. The second term ( $\int_{p_s}^{p_0} B(T(p)) d\tau$ ) is the emission of the entire atmosphere to the top. The last term ( $(1 - \epsilon_s) \tau_s \int_{p_s}^{p_0} B(T(p)) d\tau$ ) represents the downward emission from the entire atmosphere, which is reflected from the surface back to the top at the same frequency. Scattering by the atmosphere is considered to be negligible. The parameter  $\epsilon_s$  is typically 0.95 over land and 0.99 over ocean for CO<sub>2</sub> slicing wavelengths.

[8] Therefore the ratio of the deviations in cloud produced radiances ( $R$ ) and corresponding clear-sky radiances ( $R_{clr}$ ) for two spectral bands  $\nu_1$  and  $\nu_2$  viewing the same FOV are written as

$$\frac{\Delta R(\nu_1)}{\Delta R(\nu_2)} = \frac{R(\nu_1) - R_{clr}(\nu_1)}{R(\nu_2) - R_{clr}(\nu_2)} = \frac{N_{\epsilon_c(\nu_1)} \left\{ \int_{p_s}^{p_0} \tau(\nu_1, p) dB(\nu_1, p) + (1 - \epsilon_s) \tau_s(\nu_1) (B_s(\nu_1) - \int_{p_0}^{p_s} B(\nu_1, p) d\tau^\perp(\nu_1, p)) \right\}}{N_{\epsilon_c(\nu_2)} \left\{ \int_{p_s}^{p_0} \tau(\nu_2, p) dB(\nu_2, p) + (1 - \epsilon_s) \tau_s(\nu_2) (B_s(\nu_2) - \int_{p_0}^{p_s} B(\nu_2, p) d\tau^\perp(\nu_2, p)) \right\}} = \frac{N_{\epsilon_c(\nu_1)} * RM(\nu_1)}{N_{\epsilon_c(\nu_2)} * RM(\nu_2)} \quad (2)$$

where  $\epsilon_c$  represents the cloud emissivity.

[9] On the left side of equation (2), the cloudy radiances are measured from the satellite data, and clear radiances are inferred from the neighboring clear FOVs or calculated from the clear-sky temperature and moisture profiles. For two CO<sub>2</sub> sensitive spectral bands  $\nu_1$  and  $\nu_2$ , if the frequencies are close enough, the cloud emissivities have often been presumed to be equal ( $N_{\epsilon_c(\nu_1)} \cong N_{\epsilon_c(\nu_2)}$ ). However, cloud emissivity ratios calculated for thin clouds using the radiative transfer model Streamer [Key and Schweiger, 1998] suggest values deviating by 5% from one.  $RM(\nu)$  is calculated using the radiative properties of the atmosphere in the longwave CO<sub>2</sub> spectral bands given an estimate of the temperature and moisture profiles. The CTP is determined when  $|\Delta R(\nu_1) * RM(\nu_2) - \Delta R(\nu_2) * RM(\nu_1) * N_{\epsilon_c(\nu_1)} / N_{\epsilon_c(\nu_2)}|$  is minimum.

[10] Once a CTP has been determined, an ECA is evaluated from the infrared window (IRW) band data using

$$ECA = N_{\epsilon_c(w)} = \frac{R(w) - R_{clr}(w)}{R_{bd}(w) - R_{clr}(w)} \quad (3)$$

where  $w$  represents the infrared window band frequency and  $bd$  refers to blackbody.

[11] If no ratio of radiance differences between clear and cloudy skies can be reliably calculated in equation (2), because  $(R - R_{clr})$  is too small and hence within the instrument noise level, then the cloud is assumed to be opaque, and a CTP is calculated directly from the IRW band radiance observations and the clear-sky temperature profile.

[12] In this study, to evaluate the performance of the CO<sub>2</sub> slicing algorithm with surface and cloud emissivity adjustments, the IRW technique is not used in calculating CTP.

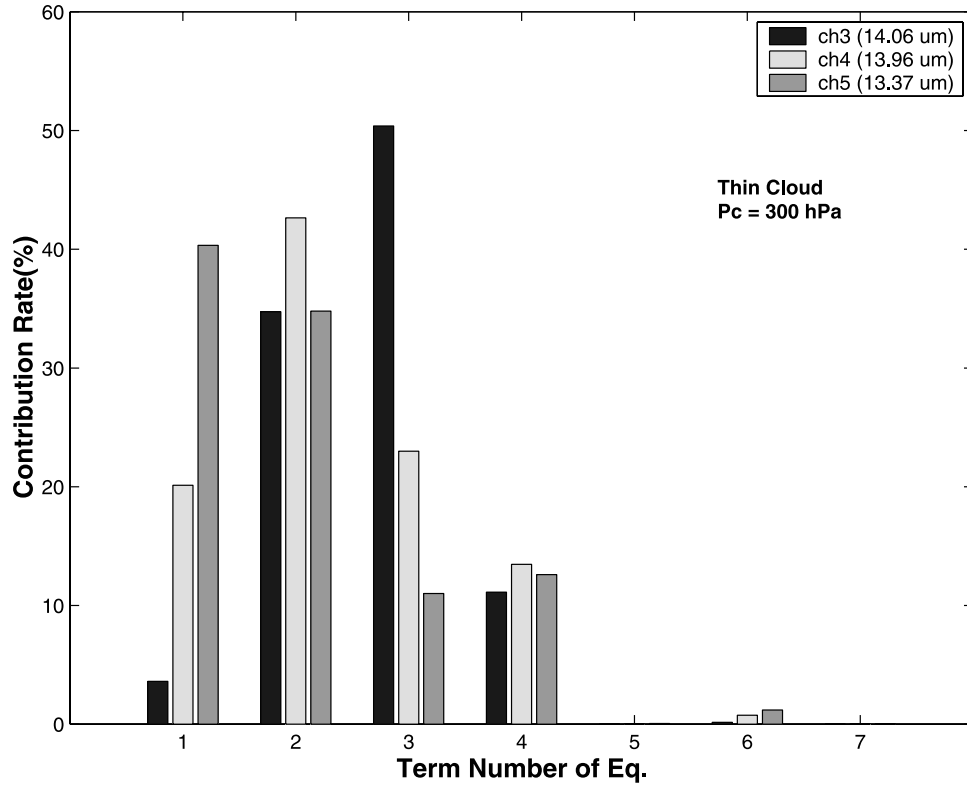


**Figure 2.** Comparisons of the contribution of each term in the RTE for high thin cloud in CO<sub>2</sub> wavelengths 14.06, 13.96, and 13.37 μm, which are GOES 8 spectral bands 3, 4, and 5, respectively. Term 1 on the *x* axis denotes the contribution from the surface; term 2 is the atmospheric contribution below the cloud; term 3 presents the atmospheric contribution above the clouds; term 4 is the emission from the cloud itself. Terms 5–7 represent the radiative contributions that are reflected at the surface to the top of the atmosphere originating from the cloud itself, below the cloud, and above the cloud, respectively.

All the cloud properties are retrieved from CO<sub>2</sub> spectral band pairs.

### 2.1. Radiation Contribution From Each Term in the RTE

[13] The upwelling radiance measured by the satellite radiometer for a cloudy atmosphere,  $R$ , is represented by

$$\begin{aligned}
 R = & \epsilon_s B_s \tau_s (1 - \epsilon_c) + (1 - \epsilon_c) \int_{p_s}^{p_c} B d\tau + \int_{p_c}^{p_0} B d\tau + \epsilon_c B_c \tau_c \\
 & + \epsilon_c B_c \tau_c (1 - \epsilon_s) \tau_s (1 - \epsilon_c) + (1 - \epsilon_s) \tau_s (1 - \epsilon_c) \int_{p_s}^{p_c} B d\tau^\downarrow \\
 & + (1 - \epsilon_c) (1 - \epsilon_s) \tau_s (1 - \epsilon_c) \int_{p_0}^{p_c} B d\tau^\downarrow
 \end{aligned} \quad (4)$$

The first term on the right-hand side of equation (4) denotes the contribution from the surface. The second and third terms are the atmospheric contribution from below and above the cloud, respectively. The fourth is the emission of the cloud itself. The fifth through seventh terms represent the radiative contributions from reflections at the surface to the top of the atmosphere originating from the cloud itself, below the cloud, and above the cloud,

respectively. A schematic of these contributions is shown in Figure 1.

[14] For high thin clouds (CTP = 300 hPa, ECA = 0.2) in a U.S. Standard Atmosphere with surface emissivity of 0.95, the percentage contribution of each term to the total radiance for the CO<sub>2</sub> bands is shown in Figure 2. The first four terms in equation (4) contribute significantly to the outgoing radiation; the last three terms do not.

### 2.2. Surface Emissivity Effects

[15] Table 1 shows that surface emissivity typically range from 0.85 and 0.99 in the longwave CO<sub>2</sub> spectral bands.

**Table 1.** Emissivities for Different Surface Types in Infrared Wavelength of 8–14 μm

Surface Type	Emissivity
Rocks	
Igneous	0.95 ~ 0.98
Metamorphic	0.96 ~ 0.98
Soils	0.97 ~ 0.98
Water	0.99
Decomposing soil litter	0.96 ~ 0.98
Vegetation	
Green foliage	0.95 ~ 0.98
Senescent foliage	0.85 ~ 0.98
Ice	0.97

**Table 2.** Spectral and Radiometric Characteristics of the MAS CO<sub>2</sub> Bands and the Equivalent GOES 8 Sounder Bands

MAS Band	Central Wavelength, μm	NEDT, <sup>a</sup> K
45	11.02	0.10
48	13.23	0.49
49	13.72	1.32
50	14.17	2.00

<sup>a</sup>NEDT represents the noise equivalent temperature change for a target at 300 K.

The CTP and ECA retrieved from the CO<sub>2</sub> slicing method with and without a surface emissivity adjustment were studied. The results show that the surface emissivity adjustment places the CO<sub>2</sub> slicing solution for high thin clouds lower in the atmosphere; a 2% surface emissivity decrease results in an increase of about 15 hPa for CTP and an increase of 1% for ECA.

### 2.3. Spectral Cloud Emissivity Effects

[16] The CO<sub>2</sub> slicing algorithm estimates CTP and ECA assuming nonscattering clouds with spectrally uniform cloud emissivity ( $\epsilon_c^i = \epsilon_c^j$ ) in the longwave CO<sub>2</sub> spectral bands. However, the cloud emissivity varies with the wavelength in 15 μm spectral region. The cloud emissivity ratio for pairs of bands ( $i, j$ )

$$E_{ij} = \frac{N\epsilon_c^i}{N\epsilon_c^j} = \frac{\epsilon_c^i}{\epsilon_c^j} \quad (5)$$

has been found to deviate by 5% from one for Streamer calculations for thin ice clouds in a U.S. Standard Atmosphere with surface emissivity fixed at 0.95. In CO<sub>2</sub> slicing calculations for high thin clouds (CTP = 300 hPa and ECA = 0.2), a 10% increase in cloud emissivity ratio was found to cause about a 35 hPa increase in CTP and a 1% increase in ECA. Increasing the cloud emissivity ratio places the cloud lower in the atmosphere and makes it thicker.

[17] Possible cloud emissivity ratios for MAS CO<sub>2</sub> bands (characteristics are shown in Table 2) observing thin high

(CTP = 300 hPa) ice clouds were calculated using the Streamer model wherein longwave ice cloud optical properties are based on Mie calculations using spherical particles at a relatively high spectral resolution. The radiative transfer model was used initially without clouds to establish a clear-sky radiance  $R_{clr}$ . An opaque cloud radiance,  $R_{bd}$ , was determined by setting all temperatures at levels below cloud level ( $p_c$ ) to the cloud temperature  $T(p_c)$ , thereby simulating an infinitesimally thin black cloud. The surface emissivity was assumed to be 0.95. Cloud emissivity was then calculated using

$$\epsilon_c^i = \frac{R^i - R_{clr}^i}{R_{bd}^i - R_{clr}^i}. \quad (6)$$

Single scattering was assumed in the calculation. The parameterization follows the methodology of *Hu and Stamnes* [1993], that depends on ice water concentration (IWC) and the effective radius (defined as the ratio of the third moment of the size distribution to the second moment) of the ice crystal size distribution. Radiances for three different IWCs (0.08, 0.04, and 0.02 g m<sup>-3</sup>) were calculated with effective radii for ice clouds being 10 μm or 20 μm.

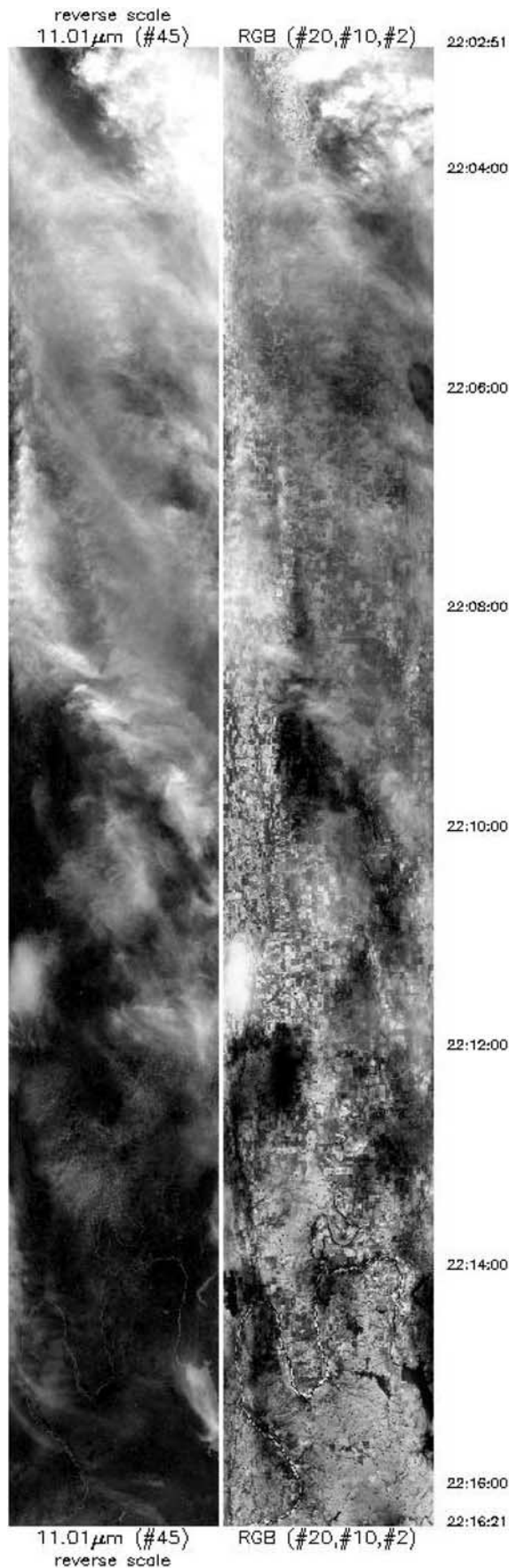
[18] For the thin cirrus cloud calculations, a single isothermal layer of small spheres was assumed. This assumption is supported by the work of *Chung et al.* [2000], who found that line by line radiative transfer calculations of small spherical (5 to 20 μm) particle thin cirrus cloud spectra matched high spectral resolution infrared interferometer measurements very well (within 1.5 K for 700 to 1300 wave numbers). Two cloud physical thicknesses, 0.25 km and 0.5 km, were studied. The calculated cloud emissivities in the MAS CO<sub>2</sub> bands and their ratios are shown in Table 3. For a fixed thickness, the emissivity depends mainly upon two parameters, the particle concentration and the cloud temperature. The concentration greatly affects the optical depth of a cloud and consequently changes the radiative properties significantly, while the cloud temperature is the fundamental source of the emitted radiation.

**Table 3.** Cloud Emissivities and Ratios for 300 hPa Ice Clouds From Streamer<sup>a</sup>

IWC, g m <sup>-3</sup>	$\epsilon_c^{45}$	$\epsilon_c^{48}$	$\epsilon_c^{49}$	$\epsilon_c^{50}$	$\epsilon_c^i/\epsilon_c^j$ Ratio		
					48/45	49/48	50/49
<i>10 μm Size Distribution for a Cloud Physical Thickness of 0.25 km</i>							
0.08	0.8616	0.9131	0.9127	0.9207	1.0598	1.0045	1.0038
0.04	0.6353	0.7060	0.7151	0.7248	1.1113	1.0129	1.0136
0.02	0.4480	0.4982	0.7248	0.5220	1.1121	1.0207	1.0265
<i>10 μm Size Distribution for a Cloud Physical Thickness of 0.5 km</i>							
0.08	0.9830	0.9938	0.9944	0.9949	1.0109	1.0006	1.0005
0.04	0.8795	0.9218	0.9262	0.9307	1.0481	1.0049	1.0048
0.02	0.7277	0.7727	0.7812	0.7914	1.0618	1.0131	1.0110
<i>20 μm Size Distribution for a Cloud Physical Thickness of 0.25 km</i>							
0.08	0.6424	0.6808	0.6914	0.7803	1.0598	1.0156	1.1286
0.04	0.4534	0.4826	0.4936	0.4466	1.0644	1.0228	0.9048
0.02	0.3515	0.3718	0.3812	0.2927	1.0578	1.0253	0.7678
<i>20 μm Size Distribution for a Cloud Physical Thickness of 0.5 km</i>							
0.08	0.8835	0.9068	0.9125	1.0000	1.0264	1.0063	1.0959
0.04	0.7324	0.7579	0.7673	0.6845	1.0348	1.0124	0.8921
0.02	0.6254	0.6454	0.6551	0.4939	1.0319	1.0150	0.7539

<sup>a</sup>The  $\epsilon_c^{45}$ ,  $\epsilon_c^{48}$ ,  $\epsilon_c^{49}$ , and  $\epsilon_c^{50}$  refer to cloud emissivity for MAS bands 45 (11.02 μm), 48 (13.23 μm), 49 (13.72 μm), and 50 (14.17 μm), respectively.





[19] Cloud emissivity ratios for the MAS CO<sub>2</sub> band pairs (48/45 or 13.2 μm/11.0 μm, 49/48 or 13.7 μm/13.2 μm, and 50/49 or 14.2 μm/13.7 μm) range from 0.75 to 1.1. For small particle cloud (particle size 10 μm), a mean cloud emissivity ratio of 1.05 works well for most of the CO<sub>2</sub> bands for most IWC. For larger particle cloud (particle size 20 μm), the emissivity ratios 48/45 and 49/48 remain well represented by 1.05, while 50/49 decreases from 1.1 to 0.75 as IWC decreases from 0.08 to 0.02 g m<sup>-3</sup>.

### 3. Validation of Adjusted CO<sub>2</sub> Slicing Algorithm Using MAS and CLS Data

[20] To evaluate the CO<sub>2</sub> slicing cloud heights obtained with a cloud emissivity adjustment, cloud data from the MAS [King *et al.*, 1996] and the CLS [Spinhrne and Hart, 1990] were compared. Both flew on the National Aeronautics and Space Administration (NASA) ER-2 during the Subsonic Aircraft Contrail and Cloud Effects Special Study (SUCCESS) field campaign in 1996. Frey *et al.* [1999] described a comparison of MAS CO<sub>2</sub> slicing with CLS cloud heights, which was considered to be “truth” value. The data are reprocessed here with the adjusted CO<sub>2</sub> slicing algorithm using a surface emissivity of 0.95 (representing the vegetated surface under the MAS flight track) and a constant cloud emissivity ratio for all spectral band pairs.

[21] As Frey *et al.* [1999] described, the MAS cloud mask [Ackerman *et al.*, 1998] was used to screen the data for the clear-sky FOVs before the CO<sub>2</sub> slicing algorithm was applied. Temperature and moisture profiles were obtained from National Weather Service (NWS) radiosonde data and were used as input to a forward radiative transfer model for computation of clear-sky radiances needed in the CO<sub>2</sub> slicing algorithm. Transmittances were determined from PFAST (Pressure-layer Fast algorithm for Atmospheric Transmittance) model [Hannon *et al.*, 1996] using appropriate MAS spectral response functions. Optically thin clouds were chosen to be those cases where a cloud and a surface signal were both present in the CLS data.

[22] Three case studies with cirrus as well as thicker clouds were found from flight tracks on 16 April 1996 over the CART (Cloud and Radiation Testbed) site. (The MAS images are available at <http://cimss.ssec.wisc.edu/success/apr16/>, and the corresponding CLS images are available at <http://virl.gsfc.nasa.gov/~success/success.html>.)

#### 3.1. Track 14 on 16 April 1996: MAS Case 1

[23] Figure 3 shows a MAS image of track 14 over Kansas and Oklahoma in the central United States on 16 April 1996 between 2202 and 2216 UTC. There are numerous high thin clouds in evidence. Single layer cloud observations from the CLS and MAS cloud retrievals for

**Figure 3.** (opposite) (left) MAS image for band 45 (11.01 μm) on track 14 on 16 April 1996. (right) Composite image from bands 2, 10, and 20. The starting and ending times for the image are 2202:51 and 2216:21 UTC. Image is from the SUCCESS homepage (<http://cimss.ssec.wisc.edu/success/apr16/>). See color version of this figure at back of this issue.

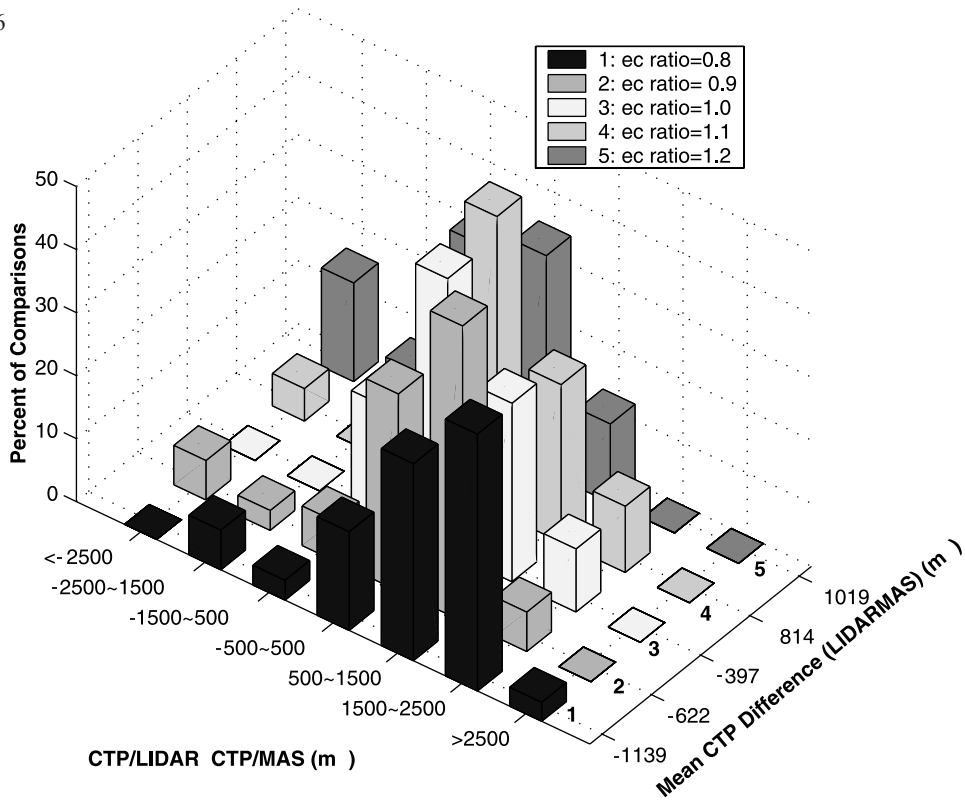


**Figure 4a.** Comparisons of cloud top heights (CTP) between from CLS and the MAS CO<sub>2</sub> slicing algorithm with different cloud emissivity ratio adjustments (0.8, 0.9, 1.0 (no adjustment), 1.1, and 1.2). The MAS data are from single layer clouds, and cloud top heights are greater than 4000 m on track 14 on 16 April 1996.

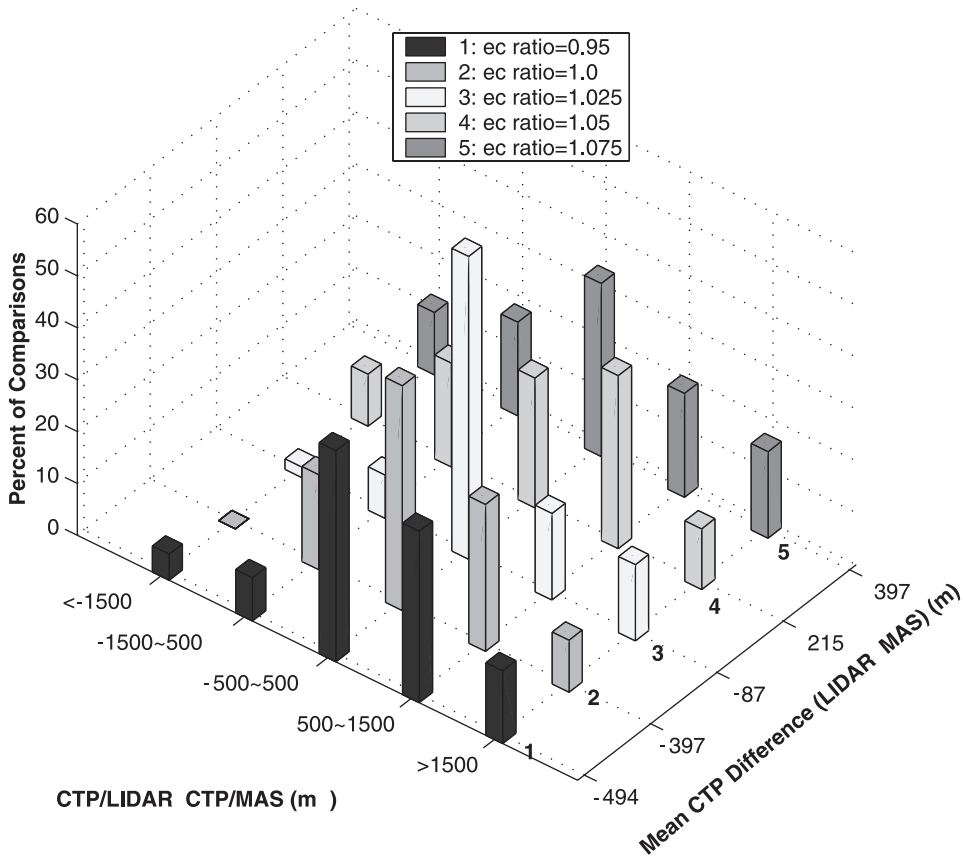


**Figure 4b.** The same as Figure 4a, but for the cloud emissivity ratios 0.95, 1.025, 1.05, and 1.075. Mean CTP difference (LIDAR - MAS) is smallest (-87 m) for cloud emissivity ratio of 1.025.

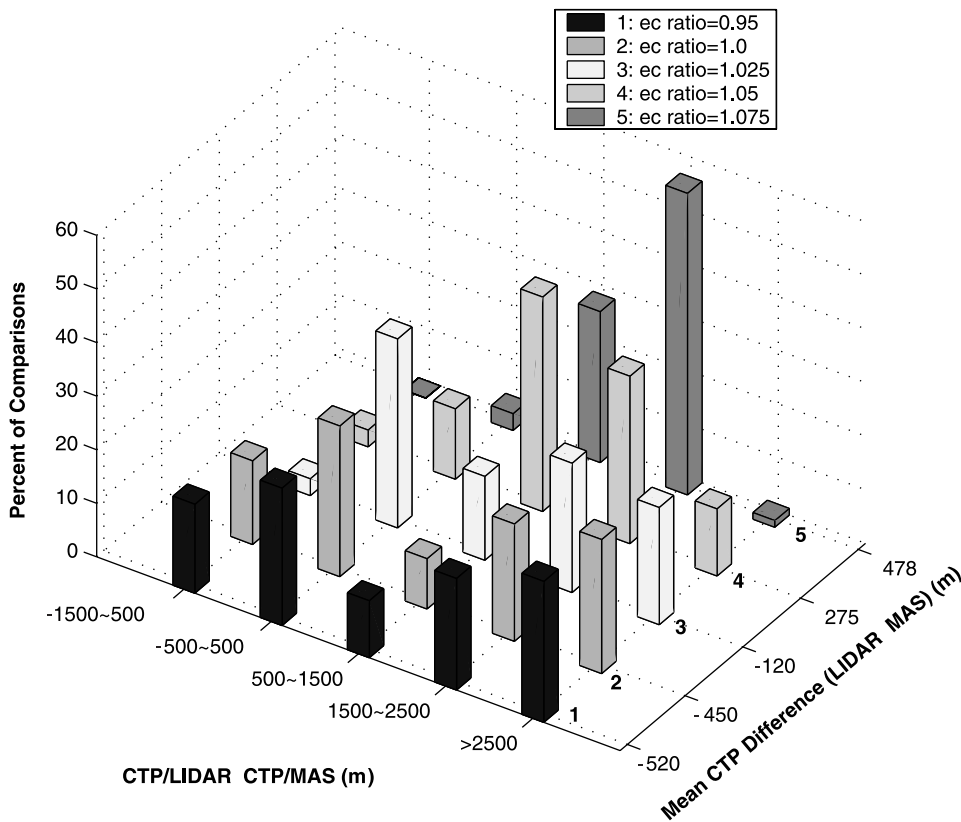


**Figure 5.** Comparisons of cloud top heights between from CLS and the MAS CO<sub>2</sub> slicing algorithm with different cloud emissivity ratio adjustments (0.95, 1.025, 1.05, and 1.075). The MAS data are from single layer clouds and cloud top heights are greater than 4000 m on track 17 on 16 April 1996. Mean CTP difference (LIDAR – MAS) is smallest (–120 m) for cloud emissivity ratio of 1.025.

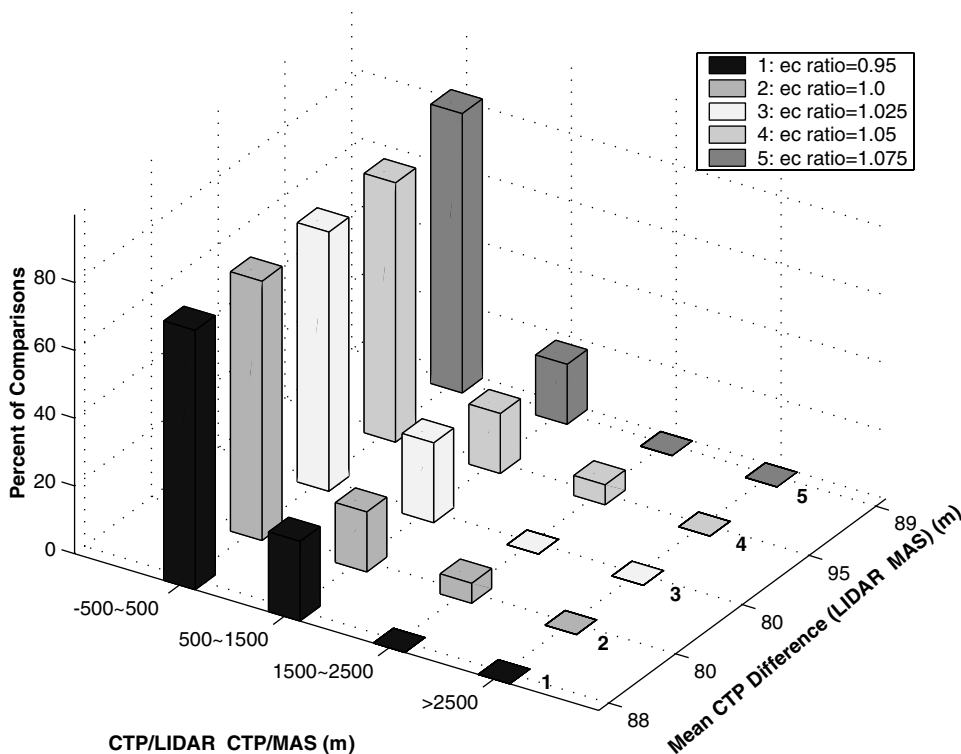


**Figure 6.** Comparisons of cloud top heights between from CLS and MAS CO<sub>2</sub> slicing algorithm with cloud emissivity ratio adjustments (0.95, 1.025, 1.05, and 1.075). The MAS data are from single layer clouds and cloud top heights are greater than 4000 m on track 3 on 16 April 1996. Mean CTP difference is not very sensitive to cloud emissivity ratio for thick clouds; all ratios show 80 to 95 m differences.

**Table 4.** Spectral and Radiometric Characteristics of the GOES 8 Sounder CO<sub>2</sub> Bands

Band	Central Wavelength, $\mu\text{m}$ (Wave Number, $\text{cm}^{-1}$ )	NEDT, <sup>a</sup> K	Purpose
Longwave			
1	14.71 (680)	1.02	stratosphere temperature
2	14.37 (696)	0.87	troposphere temperature
3	14.06 (711)	0.60	upper level temperature
4	13.96 (733)	0.40	midlevel temperature
5	13.37 (748)	0.45	low level temperature
Window			
6	12.66 (790)	0.20	total PW
7	12.02 (832)	0.13	surface temperature, moisture
8	11.03 (907)	0.10	surface temperature

<sup>a</sup>NEDT represents the noise equivalent temperature change for a 300 K target.

five ratios ( $E_{ij} = 0.8, 0.9, 1.0$  representing no adjustment, 1.1, and 1.2) are shown in Figure 4a. The distribution of cloud top height difference (CLS – MAS) is shown in 1000 m intervals; at an altitude of 10 km in a U.S. Standard Atmosphere, 500 m corresponds to  $\sim 20$  hPa. The  $\pm 500$  m difference contains the most occurrences for the ratio 1.1, which is 47% of total cases. Investigating further, results are shown for cloud emissivity ratios of 0.95, 1.025, 1.05, and 1.075 in Figure 4b. The best performance of the CO<sub>2</sub> slicing method with a cloud emissivity adjustment occurs at 1.025; 58.3% of the comparisons fall in the  $\pm 500$  m class and the mean CLS – MAS cloud height difference is  $-87$  m. Hence for this situation, the CO<sub>2</sub> slicing technique with the cloud emissivity adjustment improves the agreement with the CLS observations.

[24] Cloud emissivity ratios of 1.04, 1.01, and 0.95 for 48/45, 49/48 and 50/49 respectively, suggested by Table 3 for clouds with 20 micron particles, produced a mean CLS – MAS cloud height difference of  $-385$  m, not as good as the result with the spectrally constant 1.025 cloud emissivity ratio. Other combinations of ratios did not fare any better (likely because the sensitivity of the algorithm to these ratios is modest).

### 3.2. Track 17 on 16 April 1996: MAS Case 2

[25] Another case of thin cirrus clouds is found in track 17 on 16 April 1996 over northern Oklahoma between 2241 and 2302 UTC. The ratios of 0.95, 1.025, 1.05, and 1.075 were examined and the results are shown in Figure 5. The ratio 1.025 dominates (35.3%) in the class of  $\pm 500$  m, while the ratio 1.05 has 40% in the class of 500 to 1500 m, and has only 13% in  $\pm 500$  m. Again we find that the CO<sub>2</sub> slicing technique for thin cirrus is sensitive to the cloud emissivity ratio adjustment. The best thin cloud top heights were produced with the cloud emissivity ratio of 1.025; the mean CLS – MAS cloud top difference was  $-120$  m.

### 3.3. Track 3 on 16 April 1996: MAS Case 3

[26] Case 3 introduces thick clouds, observed in track 3 on 16 April 1996 from 1841 to 1857 UTC. The ratios of 0.95, 1.025, 1.05, and 1.075 were tested and Figure 6 shows the comparisons of cloud top height differences. There is no obvious difference between the emissivity ratios. Thick clouds are not very sensitive to the cloud emissivity adjust-

ment; all ratios produce good results with mean CLS – MAS cloud height differences between 80 and 95 m. This suggests that an adjustment to the CO<sub>2</sub> slicing algorithm that tunes the heights for thin clouds does not appear to affect the results for thick clouds adversely; other cases (not shown) have confirmed this.

### 3.4. Summary of MAS and CLS Comparisons

[27] CO<sub>2</sub> cloud top heights of thin clouds are improved with a cloud emissivity ratio adjustment to 1.025 as inferred from better agreement with CLS results. For thick clouds, cloud top heights are less sensitive to the cloud emissivity ratio adjustment and 1.025 produces good results as well. Therefore, the CO<sub>2</sub> slicing algorithm with surface and cloud emissivity adjustments appears to be a better method to determine CTP of thin clouds.

## 4. GOES 8 Case Studies

[28] The performance of the CO<sub>2</sub> slicing technique with surface emissivity and cloud emissivity adjustments was studied for two cases of GOES 8 Sounder measurements [Menzel *et al.*, 1998]. Table 4 shows the spectral bands of the GOES 8 Sounder channels used in the CO<sub>2</sub> slicing algorithm. Temperature and moisture profiles were obtained from the National Centers for Environmental Prediction (NCEP) forecast analysis. Transmittance calculations were performed using PFAST [Hannon *et al.*, 1996]. Hourly surface temperature observations from the National Weather Service (NWS) or the forecast analysis are used as the surface skin temperature. If the moisture corrected 11  $\mu\text{m}$  brightness temperature is not within 2 K of the known surface temperature, then the FOV is assumed to be cloudy and CO<sub>2</sub> cloud parameters are calculated [Schreiner *et al.*, 1993]. The IR surface emissivity is retrieved simultaneously with the atmospheric profile for clear-sky conditions [Hayden 1988]; the nearby clear-sky IR emissivity is used for the cloud retrievals.

### 4.1. GOES Case 1 on 14 February 2001

[29] In Figure 7, CTPs (in hPa ( $\times 10$ )) retrieved from the CO<sub>2</sub> slicing technique with the cloud emissivity ratio adjusted to 1.025 is superimposed on the cloud image from the GOES 8 IRW at 1346 UTC on 14 February 2001. Scatter diagrams of the differences of CTP with minus without cloud emissivity adjustment versus those without adjustment were plotted for very thin clouds with ECA less than 0.2, thin clouds with ECA between 0.2 and 0.5, thick clouds with ECA between 0.5 and 0.95, and all clouds (Figure 8). The RMS difference is 55 hPa for very thin clouds and 22 hPa for thin clouds and 12 hPa for thick clouds, with the cloud emissivity adjustment produces CTPs greater 11 hPa for very thin clouds and 8 hPa for thin clouds and 5 hPa for thick clouds. Thin clouds are more sensitive than thick clouds to the emissivity ratio adjustment. For all clouds, the cloud emissivity adjustment produces CTPs greater by approximately 5 hPa, while the RMS is approximately 20 hPa overall. Figure 9 shows the scatterplot of ECA difference of the CO<sub>2</sub> slicing algorithm with minus without nonunity cloud emissivity ratio adjustment versus ECA from the CO<sub>2</sub> slicing algorithm with unity cloud emissivity ratio. The



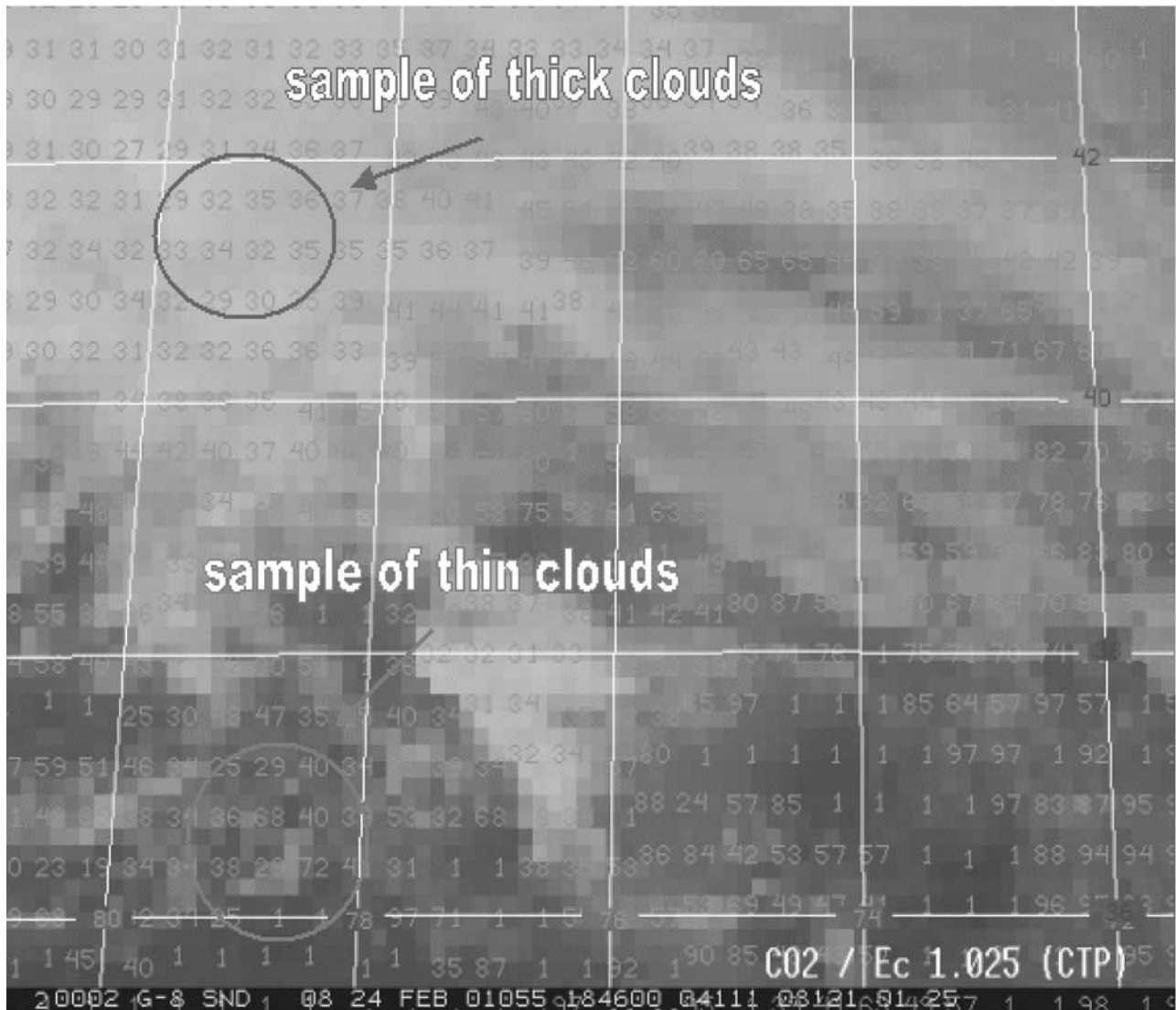


**Figure 7.** Cloud image includes both thick and thin clouds from GOES 8 1846 UTC on 24 February 2001. The number on the screen is CTPs ( $\times 10$  hPa) from the CO<sub>2</sub> slicing algorithm with cloud emissivity ratio 1.025 adjustment. The background is a GOES 8 IRW image. See color version of this figure at back of this issue.

cloud emissivity ratio adjustment increases the ECA by 0.64% and RMS is 2%, approximately.

#### 4.2. GOES Case 2 on 24 February 2001

[30] A cold frontal system moved across the central United States in case 2 at 1846 UTC on 24 February 2001. As in case 1, very thin, thin, and thick clouds were present. Investigation of CTP with cloud emissivity ratio of 1.025 versus CTPs with cloud emissivity ratio of 1.0 (no cloud emissivity adjustment) revealed similar results as the 14 February case. For very thin clouds, the mean CTP increase is 18 hPa and the RMS difference is 58 hPa. For thin clouds a RMS difference of 30 hPa is found and the mean CTP increase is 7 hPa. For thick clouds, there is no significant difference; the mean CTP increase is 5 hPa and the RMS is only 13 hPa. For all cloud types, the mean CTP increase is 5 hPa and RMS is 23 hPa, respectively; the ECA mean increase is approximately 0.14%, with RMS about 1.7%.

[31] As we expected, CTPs from the CO<sub>2</sub> slicing technique do not change significantly with cloud emissivity adjustment for thick clouds. Overall, CTP and ECA are not very sensitive to the CO<sub>2</sub> slicing with cloud emissivity adjustment; this result agrees with the calculations by *Jacobowitz* [1970], who indicated that cloud constant emissivity produces negligible errors for the CO<sub>2</sub> slicing for cloud determinations. However, for thin clouds, especially very thin clouds, there is approximately 55 hPa RMS difference of CTP between CO<sub>2</sub> slicing results with and without cloud emissivity adjustment. The thinner the clouds, the greater the difference caused by the cloud emissivity ratio. The CO<sub>2</sub> slicing with cloud emissivity ratio adjustment causes a CTP increase of 10 to 20 hPa for thin clouds.

#### 5. Summary and Conclusions

[32] The CO<sub>2</sub> slicing algorithm with surface and cloud emissivity ratio adjustments was developed to obtain

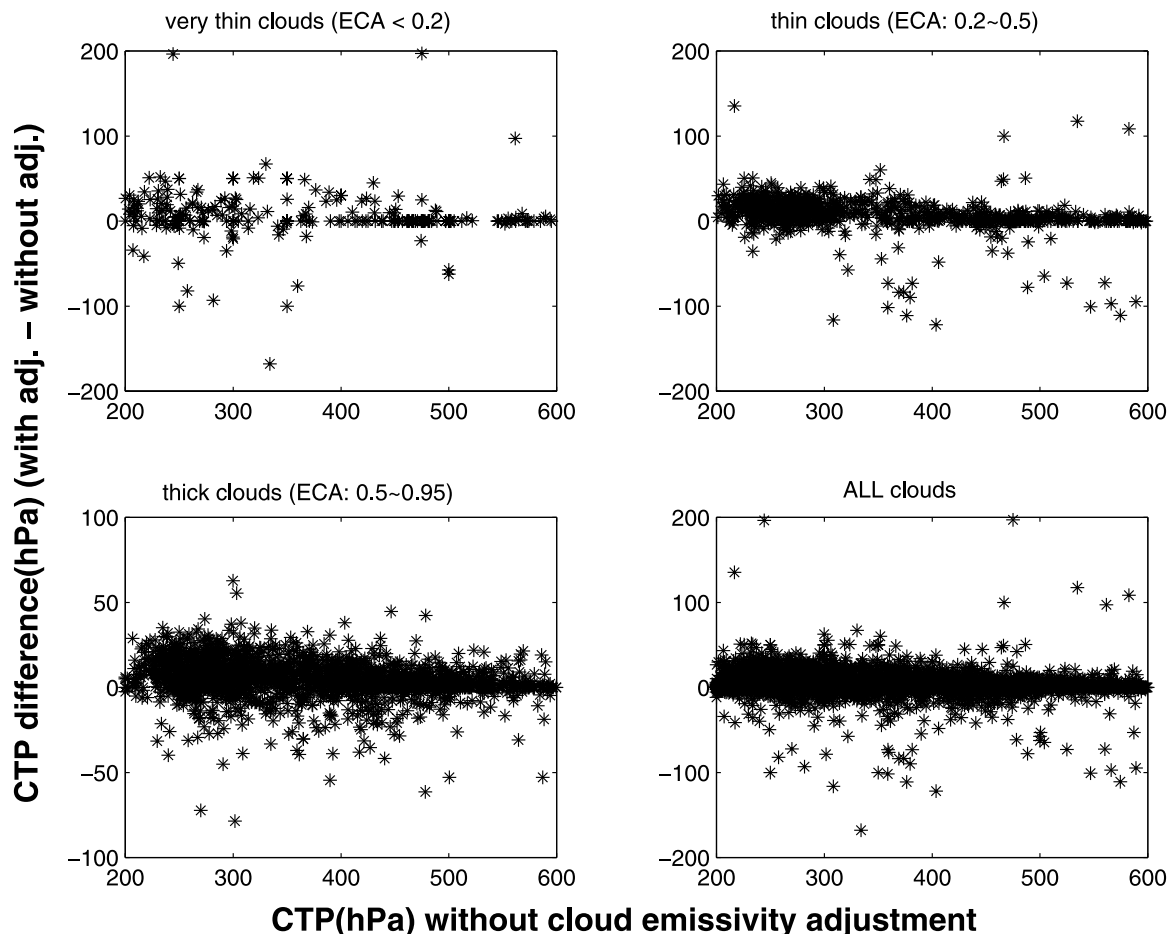


**Figure 8.** Scatterplots of CTP difference of the CO<sub>2</sub> slicing algorithm with minus without nonunity cloud emissivity adjustment versus CTP from the CO<sub>2</sub> slicing algorithm with unity cloud emissivity. The data are from the GOES 8 Sounder on 1346 UTC 14 February 2001. (top left) Comparisons for very thin clouds (ECA < 0.2) show the adjustment produces CTP greater by 11 hPa (places cloud lower in atmosphere) and RMS difference of approximately 55 hPa. (top right) For thin clouds (ECA between 0.2 and 0.5), the adjustment produces CTP greater by 8 hPa and the RMS difference is approximately 22 hPa. (bottom left) For thick clouds (ECA between 0.5 and 0.95), the adjustment produces CTP greater by 5 hPa and the RMS difference is approximately 12 hPa. (bottom right) For all cloud types, the adjustment produces CTP greater by 5 hPa and the RMS difference is approximately 20 hPa.

improved cloud top pressure and effective cloud amount. The new CO<sub>2</sub> slicing algorithm, in comparison with lidar data, showed better agreement especially for thin cirrus.

[33] Surface emissivity was found to have a small effect on the cloud properties for thin cirrus and no effect on them for thick clouds. For thin clouds, CTP increased by about 15 hPa when the surface emissivity was decreased by 2%, the associated increase in ECA was approximately 1%. Cloud emissivity ratio adjustments were found to have a somewhat larger effect on cloud properties derived from the CO<sub>2</sub> slicing, given the larger uncertainty in cloud emissivity versus surface emissivity. For thin clouds, for a cloud emissivity ratio increase of 10% (longer wavelengths divided by shorter wavelengths), the CTP increased by 35 hPa and ECA by 1%.

[34] Three case studies were presented with MAS data compared to simultaneous CLS observations during the SUCCESS field campaign. Probable cloud emissivity ratios were calculated from the radiation transfer model Streamer.

Thick clouds were found to be insensitive to the adjustments in the new CO<sub>2</sub> slicing technique. However for thin clouds, the cloud top heights were found to vary with different cloud emissivity ratios. The ratio of 1.025 was found to produce the best agreement with CLS results.

[35] The effect of the new CO<sub>2</sub> slicing method on GOES 8 Sounder data was studied. CTP increase due to surface emissivity decrease from unity was found to be approximately 5 hPa in bias and 20 hPa in RMS. Cloud emissivity ratios did not affect thick cloud retrievals; differences of CTP were less than 7 hPa. However, for very thin clouds, the CTP increase was 10–20 hPa and RMS difference was about 50 hPa; for thin clouds, the CTP increase was about 10 hPa and RMS difference was approximately 30 hPa. The new CO<sub>2</sub> slicing algorithm placed the clouds lower in the troposphere.

[36] **Acknowledgments.** This research was supported by NASA contract NAS5-31367. The authors are grateful to Timothy J. Schmit at SSEC/CIMSS, who provided significant help in the GOES Sounder data

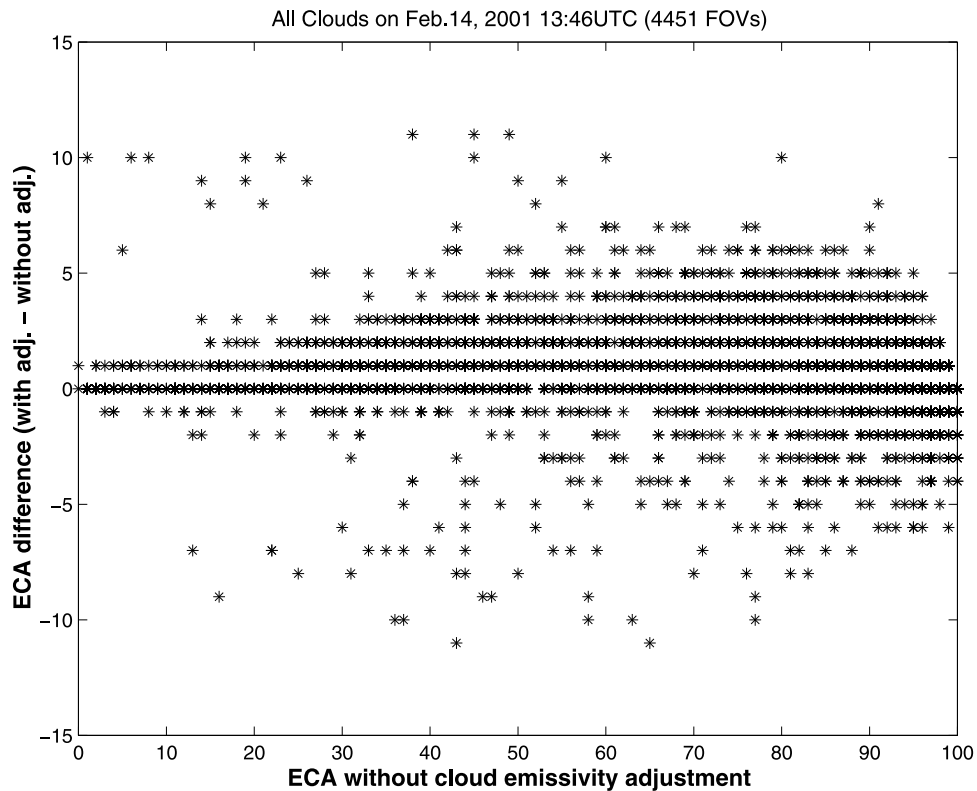


**Figure 9.** Scatterplot of ECA difference of the CO<sub>2</sub> slicing algorithm with minus without nonunity cloud emissivity ratio adjustment versus ECA from the CO<sub>2</sub> slicing algorithm with unity cloud emissivity ratio. The ECA with adjustment is about 0.64% higher, and the RMS difference is approximately 2%.

processing. The contributions of Richard A. Frey in providing the MAS and CLS data were invaluable. The authors also acknowledge the useful comments during the course of this work from Bryan Baum.

## References

- Ackerman, S. A., K. I. Strabala, W. P. Menzel, R. A. Frey, C. C. Moeller, and L. E. Gumley, Discriminating clear-sky from clouds with MODIS, *J. Geophys. Res.*, **103**, 32,141–32,157, 1998.
- Baum, B. A., and B. A. Wielicki, Cirrus cloud retrieval using infrared sounder data: Multilevel cloud errors, *J. Appl. Meteorol.*, **33**, 107–117, 1994.
- Chahine, M. T., Remote sounding of cloudy atmospheres, I, The single cloud layer, *J. Atmos. Sci.*, **31**, 233–243, 1974.
- Chung, S., S. A. Ackerman, P. F. van Delst, and W. P. Menzel, Calculations and interferometer measurements of ice cloud characteristics, *J. Appl. Meteorol.*, **39**, 634–644, 2000.
- Frey, R. A., B. A. Baum, W. P. Menzel, S. A. Ackerman, C. C. Moeller, and J. D. Spinhirne, A comparison of cloud top height computed from airborne lidar and MAS radiance data using CO<sub>2</sub> slicing, *J. Geophys. Res.*, **104**, 24,547–24,555, 1999.
- Hannon, S., L. L. Strow, and W. W. McMillan, Atmospheric infrared fast transmittance models: A comparison of two approaches, *Proc. SPIE*, **2830**, 94–105, 1996.
- Hayden, C. M., GOES-VAS simultaneous temperature-moisture retrieval algorithm, *J. Appl. Meteorol.*, **27**, 705–733, 1988.
- Hu, Y. X., and K. Stamnes, An accurate parameterization of the radiative properties of water clouds suitable for use in climate models, *J. Clim.*, **6**(4), 728–742, 1993.
- Jacobowitz, H. J., Emission scattering and absorption of radiation in cirrus clouds, Ph.D. thesis, 181 pp., Mass. Inst. of Technol., Cambridge, Mass., 1970.
- Key, J., and A. J. Schweiger, Tools for atmospheric radiative transfer: Streamer and FluxNet, *Comput. Geosci.*, **24**(5), 443–451, 1998.
- King, M. D., et al., Airborne scanning spectrometer for remote sensing of cloud, aerosol, water vapor and surface properties, *J. Atmos. Ocean. Technol.*, **13**, 777–794, 1996.
- Menzel, W. P., W. L. Smith, and T. R. Stewart, Improved cloud motion wind vector and altitude assignment using VAS, *J. Clim. Appl. Meteorol.*, **22**, 377–384, 1983.
- Menzel, W. P., D. P. Wylie, and K. I. Strabala, Seasonal and diurnal changes in cirrus clouds as seen in four years of observations with the VAS, *J. Appl. Meteorol.*, **31**, 370–385, 1992.
- Menzel, W. P., et al., Application of GOES-8/9 soundings to weather forecasting and nowcasting, *Bull. Am. Meteorol. Soc.*, **79**, 2059–2078, 1998.
- Salisbury, J. W., and D. M. D’Aria, Emissivity of terrestrial materials in the 8–14  $\mu\text{m}$  atmospheric window, *Remote Sens. Environ.*, **42**, 83–106, 1992.
- Schreiner, A. J., D. A. Unger, W. P. Menzel, G. P. Ellrod, K. I. Strabala, and J. L. Pellet, A comparison of ground and satellite observations of cloud cover, *Bull. Am. Meteorol. Soc.*, **74**, 1851–1861, 1993.
- Smith, W. L., and C. M. R. Platt, Intercomparison of radiosonde, ground based laser, and satellite deduced cloud heights, *J. Appl. Meteorol.*, **17**, 1797–1802, 1978.
- Smith, W. L., H. M. Woolf, P. G. Abel, C. M. Hayden, M. Chalfant, and N. Grody, Nimbus 5 sounder data processing system, 1, Measurement characteristics and data reduction procedures, *NOAA Tech. Memo., NESS 57*, 99 pp., Natl. Oceanic and Atmos. Admin., Silver Spring, Md., 1974.
- Spinhirne, J. D., and W. D. Hart, Cirrus structure and radiative parameters from airborne lidar and spectral radiometer observations, *Mon. Weather Rev.*, **118**, 2329–2343, 1990.
- Wielicki, B. A., and J. A. Coakley Jr., Cloud retrieval using infrared sounder data: Error analysis, *J. Appl. Meteorol.*, **20**, 157–169, 1981.
- Wylie, D. P., and W. P. Menzel, Two years of cloud cover statistics using VAS, *J. Clim.*, **2**, 292–380, 1989.
- Wylie, D. P., and W. P. Menzel, Eight years of global high cloud statistics using HIRS, *J. Clim.*, **12**, 170–184, 1999.

W. P. Menzel, Office of Research and Applications, NOAA NESDIS, University of Wisconsin-Madison, 1225 West Dayton Street, Madison, WI 53706, USA. (paulm@ssec.wisc.edu)

H. Zhang, CIMSS/SSEC, Room 415, University of Wisconsin-Madison, 1225 West Dayton Street, Madison, WI 53706, USA. (hongz@ssec.wisc.edu)

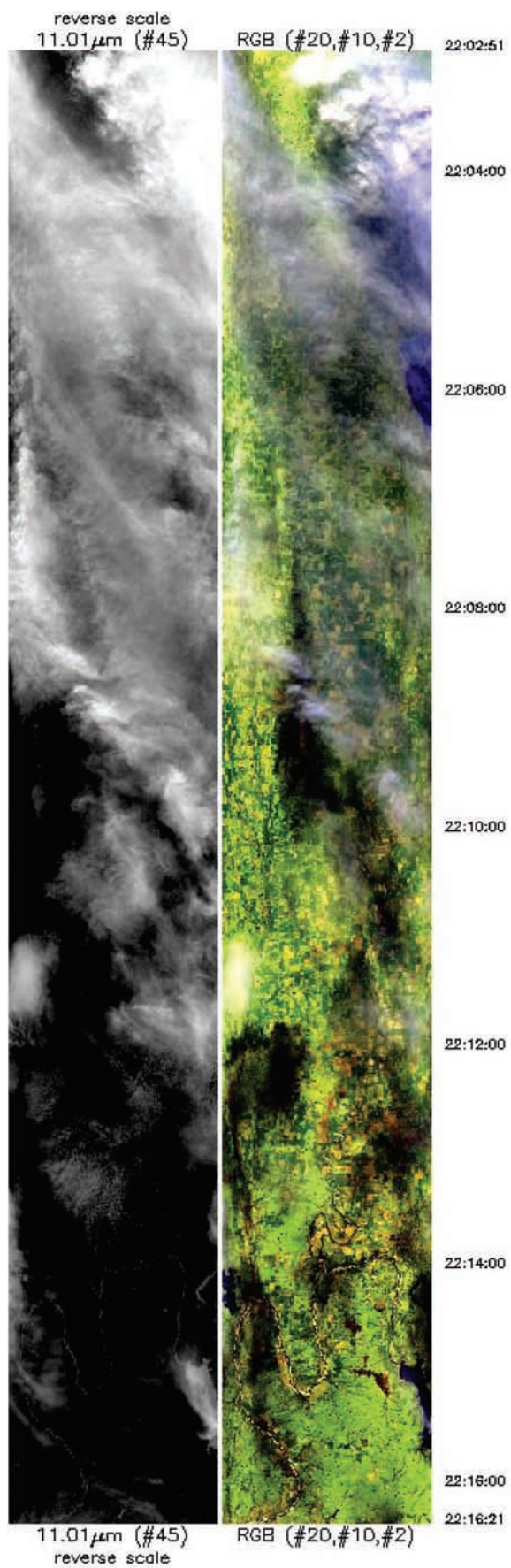


**Figure 3.** (opposite) (left) MAS image for band 45 (11.01  $\mu\text{m}$ ) on track 14 on 16 April 1996. (right) Composite image from bands 2, 10, and 20. The starting and ending times for the image are 2202:51 and 2216:21 UTC. Image is from the SUCCESS homepage (<http://cimss.ssec.wisc.edu/success/apr16/>).



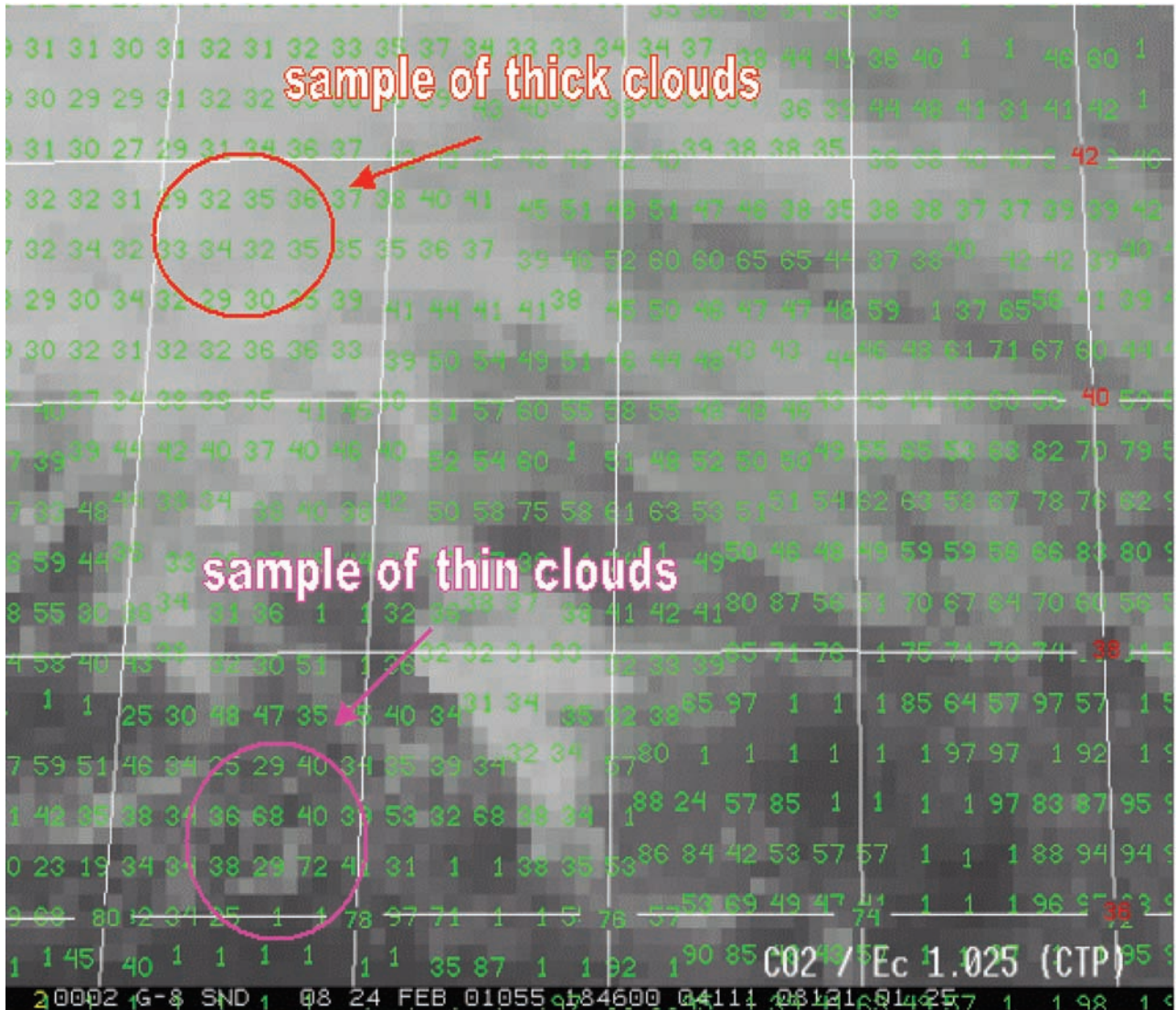


**Figure 7.** Cloud image includes both thick and thin clouds from GOES 8 1846 UTC on 24 February 2001. The number on the screen is CTPs ( $\times 10$  hPa) from the CO<sub>2</sub> slicing algorithm with cloud emissivity ratio 1.025 adjustment. The background is a GOES 8 IRW image.